Polym. Bull. (2009) 63:883–895
DOI 10.1007/s00289-009-0176-2

ORIGINAL PAPER

Effects of particle dimension and matrix viscosity on the colloidal aggregation in weakly interacting polymer-nanoparticle composites: a linear viscoelastic analysis

G. Romeo · G. Filippone · P. Russo · D. Acierno

Received: 1 July 2009 / Revised: 21 September 2009 / Accepted: 23 September 2009 /
Published online: 7 October 2009

Abstract We investigate the relation between structure and viscoelasticity of model polymer nanocomposite systems based on a mixture of spherical nanoparticles and different polymer matrices. When Brownian motions become relevant, the composites exhibit a strong time dependence of the linear visoelastic moduli, which is indicative of the three-dimensional structuring of the filler in the melt polymer. Despite the complexity of the rheological response, we show that the viscoelasticity of the samples can be rationalized by splitting it into the independent responses of the "viscous" suspending polymer melt and that of the "elastic" particle network. Besides underlying the similarities between polymer-based nanocomposites and Newtonian colloidal suspensions, our analysis is expected to be useful for understanding the behavior of other complex fluids where the elasticity of the components may be superimposed.

Keywords Polymer nanocomposites · Linear viscoelasticity · Filler network

Introduction

The mechanical properties and flow behavior of polymers can be altered by the addition of solid particles. When small amounts of inorganic fillers are mixed with a polymer, the structure of the resulting composite can be described as a suspension of particles and particle aggregates dispersed in the polymer matrix. Interactions between individual particles or aggregates and the matrix, as well as between particles, hinder the relative motion between material planes modifying both the solid-state and the melt-state behavior of the host polymer. In polymer-based

G. Romeo · G. Filippone · P. Russo · D. Acierno (✉)
Dipartimento di Ingegneria dei Materiali e della Produzione, Università di Napoli Federico II,
Piazzale V. Tecchio, 80, 80125 Naples, Italy
e-mail: acierno@unina.it

microcomposites, these effects only become significant at relatively high filler contents, that is, when the filler particles can assemble to form a network that spans over large sections of the polymer matrix [1]. Over the last 15 years the same reinforcing and thixotropic effects have been observed with the use of small amounts of inorganic nanoparticles, which has resulted in extensive research in the field of polymer-based nanocomposites [2, 3].

An important feature that characterizes the difference between nano-sized particles and microparticles used as fillers in polymers can be related to Brownian motion. In order to better understand its relevance, it is necessary to refer to the self-diffusion time τ_s of a spherical particle of radius R, given by the expression below [4]:

$$\tau_s = \frac{6\pi\eta_s R^3}{k_B T} \approx 4.5 \cdot 10^3 \cdot \eta_s R^3 \text{ s} \quad (1)$$

where η_s is the shear viscosity of the suspending medium, $k_B = 1.38 \times 10^{-23}$ J K^{-1} is the Boltzmann constant, and T is the absolute temperature. The second approximated equation applies for typical filled liquids at temperatures of order of 300 K, and the solvent viscosity η_s is expressed in Pa s and the particle radius R in μm. From Eq. 1 one predicts that in simple Newtonian fluids with η_s of order of 10^{-3} Pa s, Brownian motions occur in a timescale of order of few seconds for microparticles. On the other hand, in the case of polymer matrices with zero-shear viscosities of order of 10^3–10^4 Pa s, particles have to be a few tens of nanometers in size in order to exhibit relevant Brownian motions within similar timescales. The result is that, unlike the case of microcomposites, polymer-based nanocomposites exhibit many peculiar features of Newtonian colloidal dispersions.

When dealing with sub-micron particles dispersed in a medium, Van der Waals forces are of major importance. Attractive forces on the nanometer scale bring about the formation of particle aggregates and/or particle gels. Aggregation, gelation, and phase separation in Newtonian colloidal dispersions have been studied for decades both from a kinetic and structural point of view [5–8].

Starting from our recent results on PP/TiO_2 nanocomposites [9], in this study, we deal with the phenomenology of polymer nanocomposites with negligible polymer–particle interactions, discussing about the possibility to rationalize their viscoelastic behavior within the framework of colloidal suspensions. The first part of the work deals with the effect of particle size and matrix viscosity on the filler mobility. Because of its ability to not affect the sample structure, linear viscoelastic analysis is used as a tool for monitoring the evolutions during time of the state of dispersion of the filler in the melt. Then, we focus on the samples where the filler mobility is sufficiently high to allow three-dimensional structuring, showing that the effect of the filler on the frequency-dependent linear viscoelastic moduli can be rationalized by separating the contributions of the particle network and the matrix.

A model has been recently reported in the literature aimed at describing the complex frequency and filler volume fraction dependence of carbon nano-tubes in a polystyrene matrix [10]. However, due to the complexity of the system analyzed, the continuum mechanics nature of the model and the large number of fitting parameters, the fundamental physics underlying the origin of the rheological response of the nanocomposites remains vague. Here, we use very simple systems

allowing to easily understand the kinetics of network formation and its inhomogeneous structure.

Besides simplifying the analysis of the various timescales characterizing the behavior of polymer nanocomposites, our approach emphasizes the strong relationship existing between structure and macroscopic behavior in such complex multiphase systems.

Experimental

Nano- and microcomposites were prepared using two different polymeric matrices. The first one is a polypropylene (PP Moplen HP563N by Basell; average molecular weight $M_w = 245$ KDa; zero-shear viscosity $\eta_0 = 1.95 \times 10^3$ Pa s at 190 °C; terminal relaxation time $\tau_{PP} \approx 4 \times 10^{-1}$ s) with glass transition temperature $T_g = 6$ °C and melting temperature $T_m = 169$ °C. The second polymer matrix is an atactic polystyrene (PS, kindly supplied by Polimeri Europa). In particular, we used two PS matrices at different molecular weight, coded as PS-LOW ($M_w = 125$ KDa; $\eta_0 = 1.7 \times 10^3$ Pa s at 200 °C; terminal relaxation time $\tau_{PS\text{-}LOW} \approx 10^{-1}$ s), and PS-HIGH ($M_w = 268$ KDa; $\eta_0 = 2.1 \times 10^4$ Pa s at 200 °C; terminal relaxation time $\tau_{PS\text{-}HIGH} \approx 10^0$ s), having glass transition temperatures $T_g = 100$ °C.

Two kinds of nanoparticles were used as fillers: titanium dioxide (TiO_2 anatase nanopowder by Sigma–Aldrich; density: 3.9 g/mL; surface area: 190–290 m^2/g; average primary particles diameter $d = 15$ nm), used to prepare PP/TiO_2 nanocomposites with filler volume fractions up to $\Phi \approx 0.064$, and fumed silica (SiO_2 nanopowder by Degussa; density: 2.2 g/mL; surface area: 135–165 m^2/g; average primary particles diameter $d = 14$ nm), mixed with the two PS matrices at volume fractions up to $\Phi \approx 0.041$. PP/TiO_2 microcomposites were also prepared by using titanium dioxide microparticles (TiO_2 anatase micropowder by Sigma–Aldrich; density: 3.9 g/mL; surface area: 0.14–0.04 m^2/g; average primary particles diameter $d \approx 4$ μm).

Nano- and microcomposites were prepared by melt compounding the constituents using a co-rotating miniextruder (Minilab Microcompounder, ThermoHaake) equipped with a capillary die (diameter 2 mm). The extrusions were carried out at 190 °C and the screw speed was set to ~100 rpm, corresponding to an average shear rate of order of 50 s^{-1} inside the extrusion chamber. A feedback chamber allowed an accurate control of the residence time, which was set to 4 min for all the samples. The polymer and the filler were previously dried under vacuum for 16 h at 70 °C. The neat polymers have been extruded in the same conditions to allow accurate rheological comparison.

The morphology of the composites was examined by transmission electron microscopy (TEM mod. EM 208, Philips). The observations were carried out upon slices with thickness ~200 nm, which were randomly cut from the extruded pellets using a diamond knife at room temperature.

Rheological tests were carried out by means of either a strain-controlled rotational rheometer (ARES L.S, Rheometric Scientific) or a stress-controlled rotational rheometer (ARG2, TA Instruments), both in parallel plate geometry. The tests were

carried out using plates with diameter of 25 mm for the nanocomposites, while plates of 50 mm were used for the neat polymers because of their low viscosity. All the measurements were performed in an atmosphere of dry nitrogen. The testing temperature was $T = 190$ °C for the PP/TiO_2 samples and $T = 200$ °C for the PS/SiO_2 samples. The viscoelastic moduli display a range of strain-independence, i.e., range of linear viscoelasticity, which is dependent on the specific filler volume fraction. In order to determine the limits of the linear viscoelastic regime, oscillatory strain scans were performed upon each sample of specific volume fraction, at a fixed frequency of 0.063 rad/s. Low-frequency ($\omega = 0.063$ rad/s) time-sweep experiments were performed to study the evolution of the linear viscoelastic properties during time. The frequency-dependent viscoelastic moduli of the samples were measured by oscillatory shear frequency scans in the linear regime. In order to account for the marked sensitivity of the rheological response upon filler content, we evaluated the effective amount of filler of each sample used for the rheological experiments by thermogravimetrical analyses (TGA). The filler volume fraction Φ was estimated using the rule of mixtures:

$$\Phi = \frac{c\rho_p}{\rho_f + c(\rho_p - \rho_f)} \tag{2}$$

where c is filler weight fraction as deduced from TGA and ρ_p and ρ_f are the densities of the polymer and the filler, respectively.

Results and discussion

Untreated inorganic particles are difficult to disperse in polymer matrices due to the typically poor polymer-filler affinity [11, 12]. The hydrodynamic forces developed during extrusion can break up the large aggregates down to clusters of few tens of particles [13]. Above the melting or glass transition temperature of the polymer matrix, however, these aggregates may reassemble into bigger structures because of particle–particle attraction forces. The linear elastic (G') and viscous (G'') moduli measured at low frequencies during a small-amplitude oscillatory scan are sufficiently sensitive to changes in internal structure of the samples to make it possible to monitor such rearrangements.

In Fig. 1, we show the time dependence of G' and G'' for the PP/TiO_2 and PS-LOW/SiO_2 nanocomposites at $\Phi \approx 0.035$. The samples share the same qualitatively phenomenology: the elastic modulus increases during the earlier stage of the test until a plateau is reached. Differently, the loss modulus remains substantially constant during time. Similar results have been obtained for nanocomposites with different compositions. As the neat matrices display a constant value of both G' and G'' in time, the enhanced elasticity of the composites is solely related to the filler, and arises from its structuring during time.

The timescale for such structuring can be roughly estimated as the Smoluchowski time τ_a for two clusters to come in contact [4]. Such time depends on the self-diffusion time of each particle or cluster, as given by Eq. 1, and on the average inter-aggregates distance, which in turn is inversely proportional to the filler concentration:

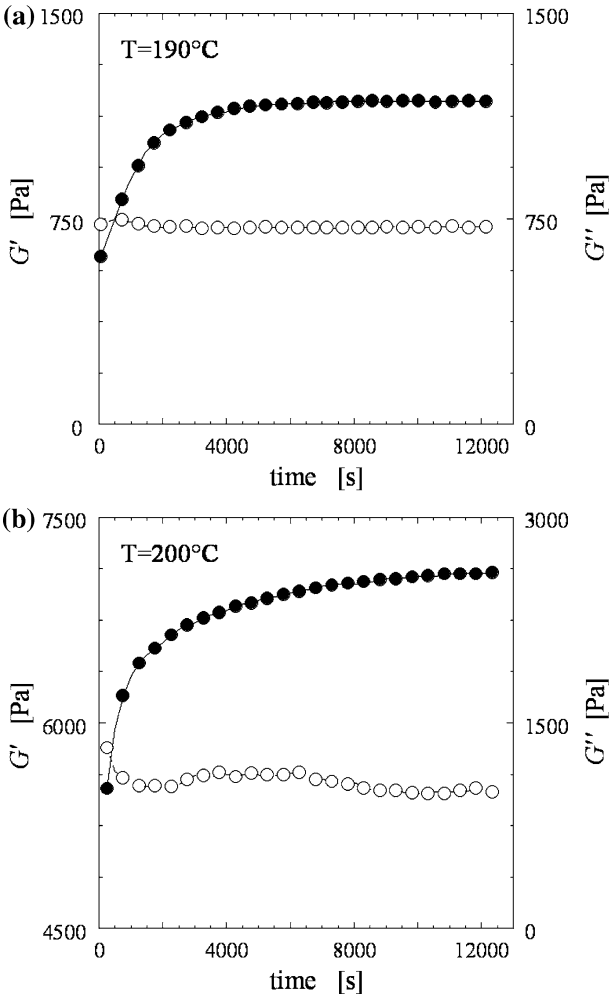

Fig. 1 Evolution of G' (*full symbols*) and G'' (*empty symbols*) at $\omega = 0.063$ rad/s for the nanocomposites PP/TiO_2 (**a**) and PS-LOW/SiO_2 (**b**). The volume fraction of both the samples is $\Phi \approx 0.035$

$$\tau_a = \frac{\pi \eta_s R^3}{\overline{\Phi} k_B T} \tag{3}$$

Here, $\overline{\Phi}$ is the effective filler volume fraction, which depends on the geometrical arrangement of primary particles inside the aggregates.

In Fig. 2, we show the typical structure of TiO_2 and SiO_2 clusters in the samples PP/TiO_2 and PS-LOW SiO_2 at $\Phi \approx 0.035$ soon after the extrusion. Since the TiO_2 aggregate (2.a) appears very compact, we can assume that, inside the aggregate, the primary titania particles are packed at $\sim 60\%$ of the apparent volume fraction Φ, which is close to random close packing. Thus, the effective filler volume fraction of the PP/TiO_2 nanocomposites can be estimated as $\overline{\Phi} \approx \Phi/0.6$. On the other hand, the

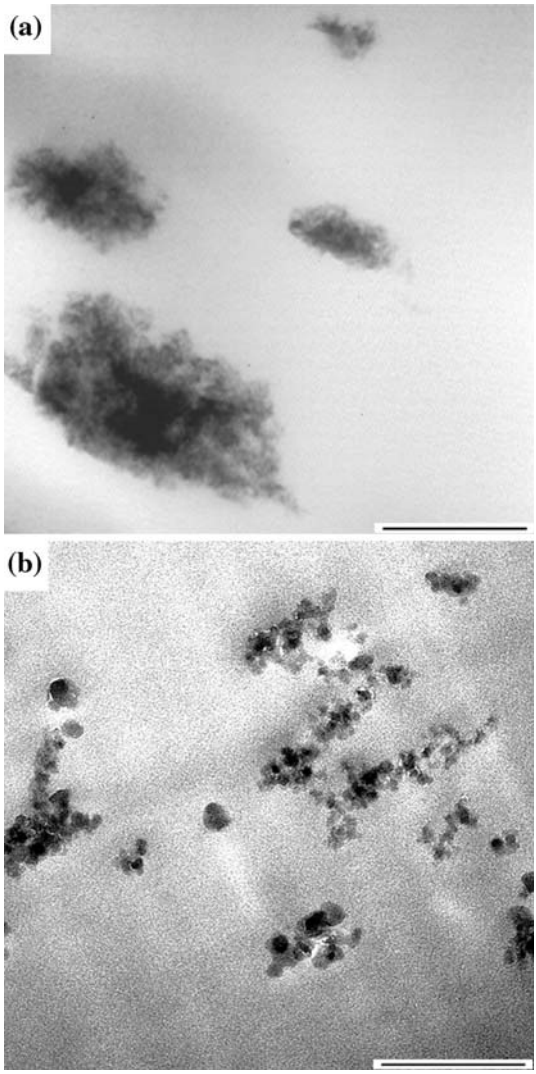

Fig. 2 TEM micrographs showing the typical structure of the clusters of TiO_2 (**a**) and SiO_2 (**b**) nanoparticles in the PP/TiO_2 and PS-LOW SiO_2 samples at $\Phi \approx 0.035$ soon after the extrusion

silica clusters shown in Fig. 2b exhibit the typical structure of fractal objects, which mass M scales with length L as $M \sim L^{d_f}$, where d_f is the fractal dimension [14]. In such a case, the effective volume fraction can be evaluated as $\overline{\Phi} = \Phi \cdot (L/d)^{3-d_f}$ [15]. Therefore, the Smoluchowski time can be roughly estimated for the two composites by assuming an average size of both TiO_2 and SiO_2 clusters of $2R \approx 100$–150 nm, as calculated from the analysis of many TEM micrographs, and by taking $d_f \approx 2.2$ as a typical fractal dimension of silica clusters [16]. Substituting these values into Eq. 2 gives $\tau_a \approx 2 \times 10^3$–$6 \times 10^3$ s for the PP/TiO_2 samples and $\tau_a \approx 10^3$–2×10^3 s for the PS-LOW/SiO_2 samples, in quite good agreement with the data shown in Fig. 1. These results support the idea that the observed increase in G' during time is related to cluster–cluster aggregation.

In order to check the validity of this deduction we can increase τ_a by increasing either the size of primary particles or clusters, R, or the viscosity of the suspending medium, η_s. According to Eq. 3, in these conditions we expect that the values of G' of the samples cannot increase significantly with time because of the much reduced particle mobility.

As a first test, we have investigated the evolutions of G' and G'' at low frequency for a PP/TiO_2 microcomposite (particle radius $R \approx 2$ μm) at $\Phi \approx 0.035$. Using Eq. 2, we expect that two micron-sized particles should come into contact after timescales of order of $\sim 10^7$ s. The results shown in Fig. 3a indicate that both moduli remain stable during aging up to $\sim 10^4$ s.

As a second test, we have monitored the viscoelastic moduli of the nanocomposite PS-HIGH/SiO_2 at $\Phi \approx 0.035$. The polymer matrix of this sample has a zero-shear

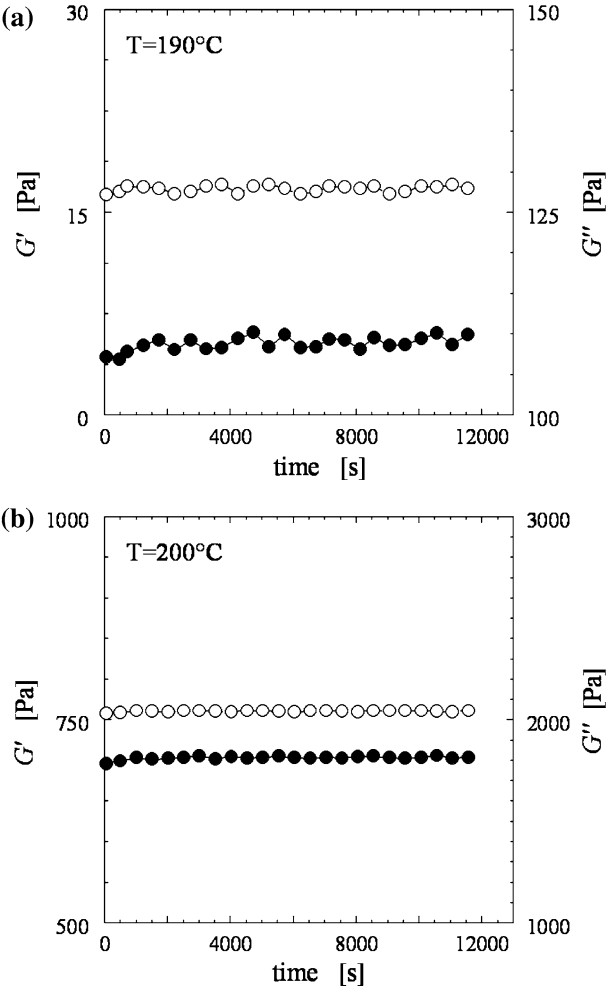

Fig. 3 Evolution in time of G' (*full symbols*) and G'' (*empty symbols*) at 0.063 rad/s for the microcomposite PP/TiO_2 (**a**) and the nanocomposite PS-HIGH/SiO_2 (**b**). The volume fraction of both the samples is $\Phi \approx 0.035$

viscosity that is about 12 times higher than that of the samples PS-LOW/SiO_2. According to Eq. 3, this means that the timescale for the formation of doublets would be of order of $\sim 10^5$ s. The results of the time-sweep experiment shown in Fig. 3b confirm that cluster assembling phenomena, if any, are negligible in the timescale of the test, and the sample keeps a predominantly viscous behavior ($G'' \gg G'$).

In order to directly compare the state of dispersion of SiO_2 nanoparticles in the two matrices with different viscosity, we performed TEM analysis upon the samples PS-LOW/SiO_2 and PS-HIGH/SiO_2 at $\Phi \approx 0.021$. The micrographs before and after a 3-h quiescent ageing at 200 °C are compared in Fig. 4.

Irrespective of the matrix viscosity, both samples exhibit a comparable microstructure after the extrusion, consisting of small aggregates homogenously distributed on microscale (Fig. 4a, c). After ageing under quiescent conditions the small clusters in the low-viscosity matrix build up into larger aggregates forming an inhomogeneous microstructure (Fig. 4b). Conversely, neither the cluster dimensions nor their state of

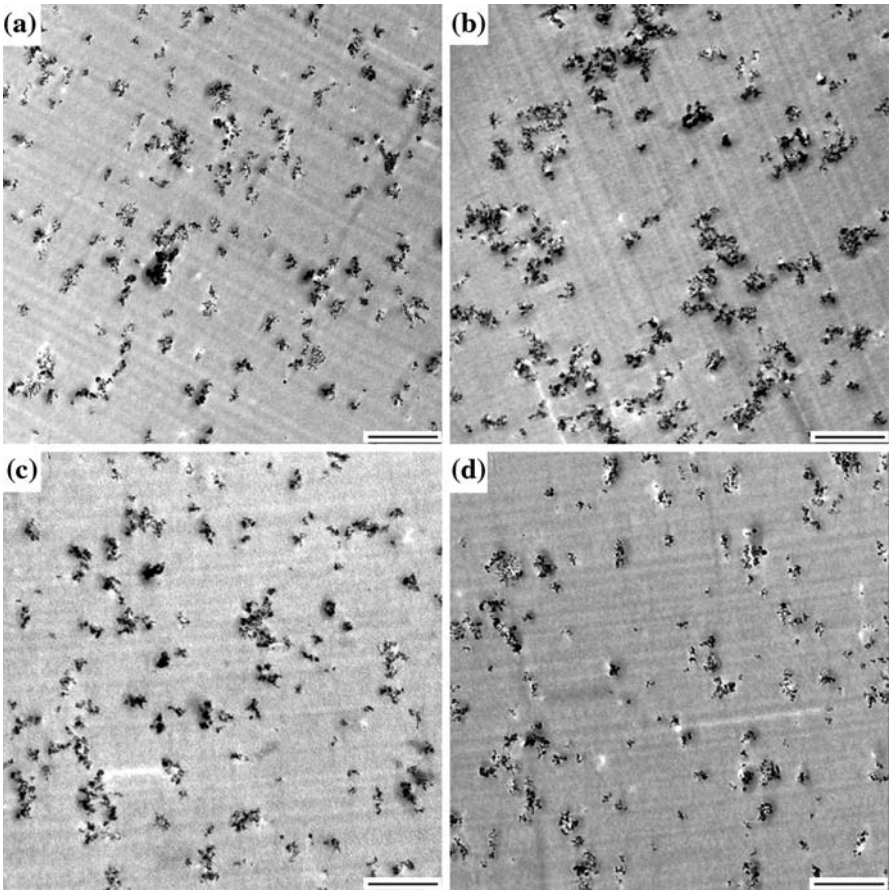

Fig. 4 TEM micrographs of PS-LOW/SiO_2 (**a**, **b**) and PS-HIGH/SiO_2 (**c**, **d**) before (**a**, **c**) and after (**b**, **d**) a 3 h annealing at $T = 200$ °C. The filler volume fraction of both the samples is $\Phi \approx 0.021$. The *scale bars* represent 500 nm

dispersion on microscale significantly change for the sample PS-HIGH/SiO_2 during quiescent ageing (Fig. 4c, d) due to the high viscosity of the polymer matrix.

Particle rearrangements may give rise to hierarchical structures consisting of branched aggregates or, eventually, a space-spanning filler network with a significant effect on the frequency response of the sample [9, 12, 15, 17]. In Fig. 5a, we compare the frequency dependence of G' and G'' for two PP/TiO_2 samples filled with micro- and nanoparticles at equal volume fraction $\Phi \approx 0.035$.

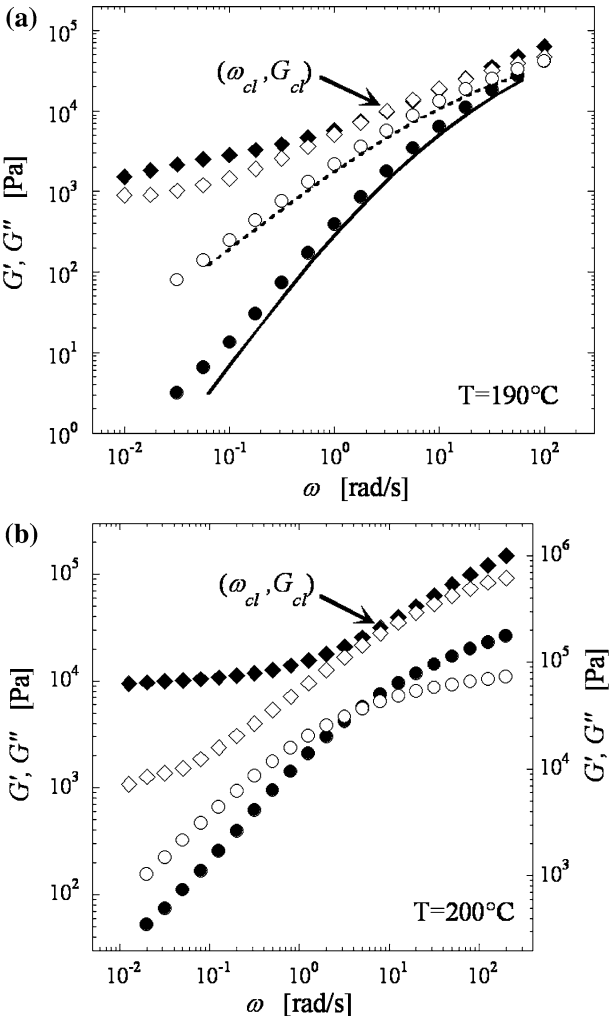

Fig. 5 **a** G' (*full symbols*) and G'' (*empty symbols*) for the samples PP/TiO_2 at $\Phi \approx 0.035$ filled with micrometric (*circles*) and nanometric (*diamonds*) particles. Solid and dashed lines represent, respectively, the elastic and viscous modulus of the neat PP. **b** G' (*full symbols*) and G'' (*empty symbols*) for the samples PS-LOW/SiO_2 (*diamonds, left axis*) and PS-HIGH/SiO_2 (*circles, right axis*) at $\Phi \approx 0.035$. The *arrows* indicate the additional crossover point characterizing the samples in which the filler form a three-dimensional network

In both cases, the matrix dictates the viscoelastic behavior at high-frequencies. In any case, while the presence of microparticles has a negligible effect on the response of the composite relatively to the neat polymer, the nanoparticles have a significant effect on the low-frequency viscoelastic moduli of the material, in particular the elastic one. The flattening of G' curve at long timescales is a general feature for different types of polymer nanocomposites [18, 19]. This behavior, however, does not arise from an effect of particle size but from particle mobility. In order to provide the evidence of this deduction, we compare in Fig. 5b the frequency response of the 3-h aged samples PS-LOW/SiO_2 and PS-HIGH/SiO_2 at the same filler volume fraction $\Phi \approx 0.035$. The nanocomposite with high viscosity matrix displays a liquid-like behavior at low frequencies reminiscent of the behavior of the neat polymer (not shown). From the observations on the TEM images and the aging curves, we may conclude that when the filler is unable to assemble into three-dimensional structures, the viscoelastic response remains essentially unaltered relatively to that of the polymer. Conversely, the PS-LOW/SiO_2 sample displays a clear low-frequency plateau of G'. As a result, the elastic modulus becomes much higher than the viscous modulus down to the smallest frequencies investigated. This plateau is indicative of the presence of a space-spanning filler network formed during ageing which is able to store elastic energy for times much longer than the relaxation time of the polymer molecules [9, 11, 12].

To summarize, the viscoelastic response of a filled polymer is greatly affected by particle mobility. When the characteristic diffusion time of the particles and/or aggregates resulting from the extrusion process is too high, the filler is unable to rearrange, and only produce a small perturbation of the composite viscoelastic response. Conversely, when mobility of the inorganic phase is high enough, random motion, and attractive particle–particle forces lead to the structuring of the primary aggregates, eventually resulting into the formation of a whole space-spanning filler network. Since this network exhibits the connotation of an elastic solid, a drastic slowing down of the relaxation dynamics occurs at low frequencies.

In order to examine the effect of the particle content on the viscoelastic behavior of the composites, in this section we focus on the frequency dependence of G' and G'' of samples in which the filler rearranges within experimentally accessible timescales into a space-spanning network. At low frequencies all samples display a pseudo-solidlike behavior, i.e., the G' values greater than G'' values and a very weak dependence on the oscillation frequency. As a consequence, a further intersection between G' and G'' curves is observed at lower frequencies, in addition to that at $\omega \approx 10^2$ rad/s, which is related to the relaxation time of the polymer matrices. As an example, the additional crossover is indicated by the arrows in Fig. 5a, b for the samples PP/TiO_2 and PS-LOW/SiO_2 at $\Phi \approx 0.035$. Since the filler mainly affects the elastic component, G' increases with Φ more rapidly than G''. Consequently, the frequency, ω_{cl}, and the modulus, G_{cl}, at the additional crossover both increase with increasing filler content.

In spite of the non-Newtonian feature of the polymer matrices, we observe that this phenomenology is reminiscent of the behavior of attractive colloidal gels in a low-viscosity Newtonian matrix [5, 17]. In these systems, the Φ-dependence of G' scales along the fluid viscosity η_s as a simple consequence of the increased number

of particles contributing to the filler network. Similarly, in our nanocomposites characterized by weak polymer–filler interactions we expect that the main contribution to the elasticity of the nanocomposites stems from the particle aggregates, representing the building elements of the filler network. Interspersed throughout this structure is the polymer, which has an intrinsic filler-independent viscoelastic behavior that mixes with the network dynamics, giving rise to complex ω- and Φ-dependence of G' and G''. However, in view of the difference in temporal relaxation scales, the viscoelasticity of the samples can be split into the independent responses of the elastic particle network, primarily dependent on filler content, and governing the long time scale response, and that of the viscous medium, which dominates the high-frequency behavior. Therefore, the additional low-frequency crossover can be interpreted as the point at which the network elasticity, represented by G_{cl}, equals the viscous contribution of the polymer. As a consequence, we expect that the appropriate scaling of the moduli at different Φ should lead to the shifting of the curves onto a single pair of master-curves. According to the physical picture proposed, the scaling was done by shifting the curves both horizontally and vertically using as shift factors $a = 1/\omega_{cl}$ and $b = 1/G_{cl}$, respectively [9].

The resulting master-curves are shown in Fig. 6 for both the PS-LOW/SiO_2 and PP/TiO_2 nanocomposites. The scaling has been performed for the samples with a clear pseudo-solidlike behavior, which is indicative of the existence of a space-spanning filler network. The scaled moduli lie on top of each other in about five decades of frequency, corroborating the validity of our approach. Deviations are observed for the viscous modulus at high scaled frequencies. This is due to the non-Newtonian feature of the polymer matrices, whose relaxation modes are independent on filler content and, as a consequence, cannot be scaled using the adopted approach.

Once the master-curves are built, the differences between elasticity and dynamics of the PP/TiO_2 and PS-LOW/SiO_2 samples become evident. The TiO_2 network displays a slow relaxation dynamics with $G' \sim \omega^{0.3}$. Conversely, the SiO_2 network is characterized by a frequency-independent elastic modulus at low frequency, which emphasizes its truly solid-like feature. These dynamic discrepancies are related to the differences in network structures formed in the two composites. Note that the TEM images reported in the insets of Fig. 6 show that the TiO_2 nanoparticles are assembled into dense clusters, which mobility is presumably slowed down by the surrounding aggregates. In fact, the transient character of such a network clearly emerges as a glassy-like decrease of G', which reflects the internal rearrangements of the TiO_2 clusters [9]. Conversely, the SiO_2 nanoparticles form a tenuous, fractal network of sub-micron sized, branched flocs interspersed within the host PS.

Conclusions

The effect on the melt-state linear viscoelastic behavior of small amounts of particles weakly interacting with the polymer matrix has been investigated for different kinds of polymer-based composites. The filler mobility in the melt

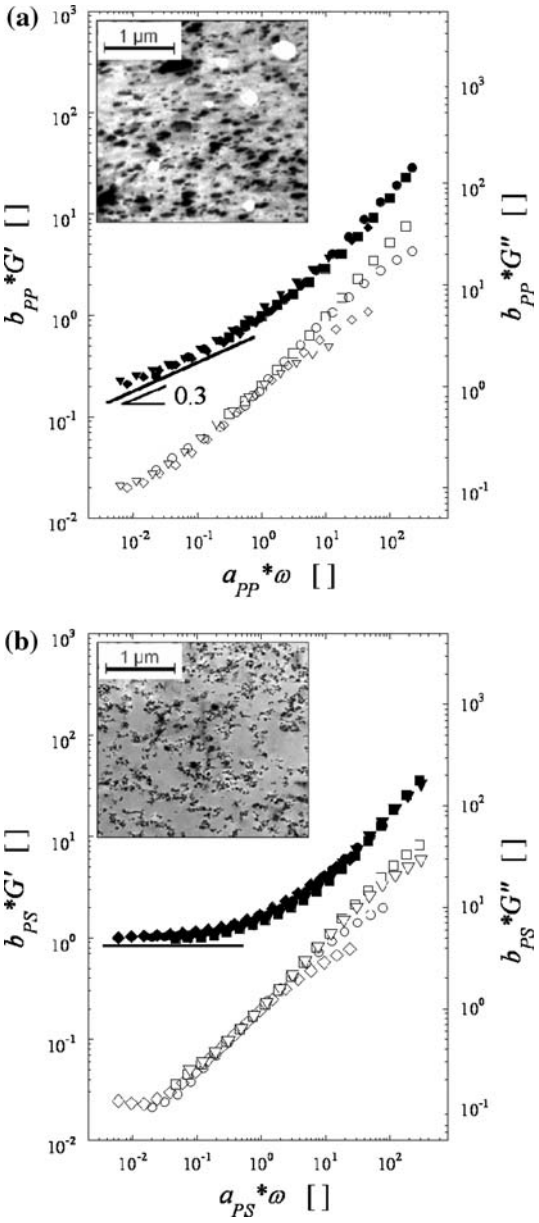

Fig. 6 Master-curves of G' (*full symbols, left axis*) and G'' (*empty symbols, right axis*) for the systems PS-LOW/SiO_2 (**a**) and PP/TiO_2 (**b**) obtained by scaling the moduli of nanocomposites at different composition. The volume fractions of the scaled curves are: (a) 0.022 (*squares*), 0.029 (*circles*), 0.03 (*diamonds*), 0.041 (*inverse triangles*), and (b) 0.034 (*squares*), 0.038 (*circles*), 0.045 (*diamonds*) and 0.064 (*inverse triangles*). TEM micrographs shown in the *insets* a and b represent the microstructures of PP/TiO_2 and PS-LOW/SiO_2 samples, respectively, both at $\Phi \approx 0.035$

polymer, depending on both the particle size and the viscosity of the suspending medium, represents the key factor for the three-dimensional structuring of the solid phase. Once formed, the network elasticity mixes with the intrinsic viscoelastic response of the polymer matrix giving rise to a complex rheological response. However, we have shown that the contributions of filler network and suspending medium are decoupled due to the weak polymer–particle interactions and the

differences in temporal relaxation scales. This allows building a master-curve by scaling the moduli of composites at different composition along the matrix viscosity with respect to the network elasticity. The employed approach, working for systems characterized by different structure of the filler network, clarifies the various timescales of the nanocomposites and makes evident the strict relationships between mesostructure and macroscopic properties in complex systems such as polymer-based nanocomposites.

References

1. Vinogradov GV, Malkin AY, Plotnikova EP, Sabsai OT, Nikolayeva NE (1972) Viscoelastic properties of filled polymers. Int J Polym Mater 2:1
2. Usuki A, Kojima Y, Kawasumi M, Okada A, Fukushima Y, Kurauchi T, Kamigaito O (1993) Synthesis of nylon 6-clay hybrid. J Mater Res 8:1179–1184
3. Kojima Y, Usuki A, Kawasumi M, Okada A, Fukushima Y, Kurauchi T, Kamigaito O (1993) Mechanical properties of nylon 6-clay hybrid. J Mater Res 8:1185–1189
4. Russel WB, Saville DA, Schowalter WR (1989) Colloidal dispersions. Cambridge University, Cambridge
5. Trappe V, Prasad V, Cipelletti L, Segrè PN, Weitz DA (1991) Jamming phase diagram for attractive particles. Nature 411:772–775
6. Segrè PN, Prasad V, Schofield AB, Weitz DA (2001) Glasslike kinetic arrest at the colloidal-gelation transition. Phys Rev Lett 86:6042–6045
7. Cipelletti L, Manley S, Ball RC, Weitz DA (2000) Universal aging features in restructuring of fractal colloidal gels. Phys Rev Lett 84 10:2275–2278
8. Mason TG, Weitz DA (1995) Linear viscoelasticity of colloidal hard sphere suspensions near the glass transition. Phys Rev Lett 75:2770–2773
9. Romeo G, Filippone G, Fernández-Nieves A, Russo P, Acierno D (2008) Elasticiy and dynamics of particle gels in non-Newtonian melts. Rheol Acta 47:989–997
10. Kota AK, Cipriano BH, Powell D, Raghavan SR, Bruck HA (2007) Quantitative characterization of the formation of an interpenetrating phase composite in polystyrene from the percolation of multi-walled carbon nanotubes. Nanotechnology 18:505705
11. Acierno D, Filippone G, Romeo G, Russo P (2007) Rheological aspects of PP-TiO2 nanocomposites: a preliminary investigation. Macromol Symp 247:59–66
12. Acierno D, Filippone G, Romeo G, Russo P (2007) Dynamics of stress bearing particle networks in poly(propilene)/alumina nanohybrids. Macromol Mater Eng 292:347–353
13. Baird DG, Collias DI (1995) Polymer processing principles and design. Butterworth-Heinemann, Burlington
14. Weitz DA, Oliveira M (1984) Fractal structures formed by Kinetic aggregation of aqueous gold colloids. Phys Rev Lett 52:1433–1436
15. Wolthers W, van den Ende D, Bredveld V, Duits MHG, Potanin AA, Wientjens RHW, Mellema J (1997) Linear viscoelastic behavior of aggregated colloidal dispersions. Phys Rev E 56:5726–5733
16. Kammler HK, Beucage G, Mueller R, Pratsinis SE (2004) Structure of flame-made silica nanoparticles by ultra-small-angle X-ray scattering. Langmuir 20:1915–1921
17. Trappe V, Weitz DA (2000) Scaling of the viscoelasticity of weakly attractive particles. Phys Rev Lett 85:449–452
18. Krishnamoorti R, Yurekly K (2001) Rheology of polymer layered silicate nanocomposites. Curr Opin Colloid Interface Sci 6:464–470
19. Ren J, Silva AS, Krishnamoorti R (2000) Linear viscoelasticity of polystyrene-polyisoprene block copolymer based layered-silicate nanocomposite. Macromolecules 33:3739–3746